Vision Research 50 (2010) 2048–2054

Contents lists available at ScienceDirect

Vision Research

journal homepage: www.elsevier.com/locate/visres

The polarization sense in human vision

Albert Le Floch [a,b,c], Guy Ropars [a,b,*], Jay Enoch [d], Vasudevan Lakshminarayanan [e,f,g]

[a] Laboratoire de Physique des Lasers, Université de Rennes 1, 35042 Rennes cedex, France
[b] Université européenne de Bretagne, 5 boulevard Laënnec, 35000 Rennes, France
[c] Laboratoire de Chimie et Photonique Moléculaires, unité CNRS 6510, Université de Rennes 1, 35042 Rennes cedex, France
[d] School of Optometry, University of California, Berkeley, CA 94720, USA
[e] School of Optometry, University of Waterloo, Waterloo, Ontario, Canada N2L 3G1
[f] Department of Electrical and Computer Engineering, University of Waterloo, Waterloo, Ontario, Canada N2L 3G1
[g] Department of Physics and Astronomy, University of Waterloo, Waterloo, Ontario, Canada N2L 3G1

ARTICLE INFO

Article history:
Received 24 July 2009
Received in revised form 10 April 2010

Keywords:
Polarization
Haidinger's brushes
S cone
Dominance
Fovea centralis

ABSTRACT

Unlike humans, numerous animals are differentially sensitive to the vector orientation of linearly polarized light. However as early as 1844 Haidinger noted that weak blue–yellow brushes appear, centered on the fovea, when the sky is observed through a slowly rotating polarizer. Different models have been proposed to try to understand this phenomenon, but the precise mechanism remains unknown and the polarization unexploited. We suggest that when Fresnel's laws are applied to the unguided oblique rays, that the cylindrical geometry of the blue cones in the fovea along with their distribution induces an extrinsic dichroism and could explain why the human eye is sensitive to polarization. We have constructed an artificial eye model system using the same laws and were able to photograph the appearance of entoptic-like blue-dark brushes, confirming the observations and our mathematical simulations. Moreover, our *in vivo* and *in vitro* tests show that in addition to the usual 3 s fading time measured using a stationary stimulus, there exists for this entoptic image a short extra creating and erasing time of about 0.1 s, using a dynamical stimulus. We have also found that, surprisingly, the rotating pattern is more regular and symmetrical with one of our two eyes around a more circular blue cone-free area, the dominant eye. Our results suggest that the polarization sense can provide important information in many areas that remain to be explored.

1. Introduction

Vision is exquisitely complex and rooted in diverse areas of science, such as optics, photochemistry and neurobiology. The aim of all invertebrate and vertebrate eyes is to gather information from the ambient electromagnetic waves. These waves possess not only two scalar properties, an amplitude and a frequency, which are widely exploited, but also a vector character, namely the polarization. There is an abundance of linearly or partially polarized light in natural environments due to reflections and refractions at different dielectric interfaces, as well as due to scattering. On Earth in particular, the Rayleigh scattering of the blue and near ultraviolet parts of the spectrum of sunlight by the atmosphere provides us with E-vector patterns over the entire celestial hemisphere depending upon the position of the sun. Since the pioneering work of von Frisch (1967) about 60 years ago, which showed that bees are sensitive to these patterns, remarkable discoveries have been made in the domain of polarization cues used by animals (Dacke et al., 2003; Heinze & Homberg, 2007; Wehner & Müller, 2006). This polarization sensitivity of animals exists in *regularly* organized opsins inserted in different types of compound or camera-type eyes. It is used for many functions such as orientation, navigation, and biological signalling. However, although humans are generally oblivious to it, a few years after the description by Malus of polarization by reflection in 1808, the first observation of human polarization sensitivity was made by Haidinger (1844). During a century and a half there have been many attempts (summarized in Horwáth & Varjú, 2004; von Helmholtz, 1962) to explain this polarization effect in human eyes with their *randomly* aligned chromophores, but to this day the mechanism remains unknown and the polarization sense largely unexploited although this phenomenon is used in ophthalmology to correct amblyopia. Apart from the anisotropies of the cornea, the Henle fibers or the lens (Brewster, 1859) most models are based on either a possible radial or tangential arrangement of absorbing elongated yellow pigments in the macula. Unfortunately, a radial alignment of anisotropically absorbing molecules along the nerve fibers which may be expected for highly elongated pigments, would lead to reversed brush colors. Tangential alignment of the molecules orthogonally to the fibers would lead to the correct colors, but are unexpected and has never been experimentally observed (Raman, 1965). Moreover, in the

* Corresponding author.
E-mail address: guy.ropars@univ-rennes1.fr (G. Ropars).

0042-6989/$ - see front matter © 2010 Elsevier Ltd. All rights reserved.
doi:10.1016/j.visres.2010.07.007

human eye unlike in animal eyes, the intrinsically dichroic cone chromophores themselves are randomly-aligned in the cone disk membranes and so lead to a spatially unresolved response of the retina whatever the direction of light polarization. We suggest here that the phenomenon originates in the transmission of oblique light subject to Fresnel's laws (Born & Wolf, 1999) in the specific blue-cone distribution in the fovea (Bumsted & Hendrickson, 1999; Cornish, Hendrickson, & Provis, 2004; Curcio et al., 1991; Wald, 1967), while the cone chromophores and transduction processing govern the fast dynamics of the phenomenon.

2. Model and simulations

2.1. Characteristics of Haidinger's brushes

The main characteristics of Haidinger's brushes can be observed when we simply look at the sky through a slowly rotating polarizer. We see a blue–yellow propeller-like pattern subtending a visual angle of about 3° centered on the fovea, the direction of the light polarization being parallel to the blue axis and perpendicular to the yellow axis. This pattern fades in a few seconds when the rotation is stopped. The image does not correspond to any real object and cannot be photographed. This entoptic property of the pattern complicates the analysis, the only stimulus being the polarization of the light entering the pupil. One main property first noted by Stokes (Stokes, 1883) is that a deep blue glass gives brushes of remarkable intensity with a blue-dark contrast. We have verified that a cobalt-doped filter with a bandwidth from 300 to 500 nm, centered at 380 nm, provides optimum contrast, while above 500 nm, with green, yellow and red filters no pattern exists whatever the light level. The short-wavelength sensitive blue cones seem to play a crucial role. We will perform most of our *in vivo* tests with only blue light, leading to contrasted blue-dark brushes appearing in place of the blue–yellow brushes observed in the presence of white light, as confirmed later by our model.

2.2. The blue-cone mosaic

Let us consider the cone mosaic in the center of the human eye fovea (Osterberg, 1935; Oyster, 1999; Polyak, 1941; Rodieck, 1998). The cone distribution on the fovea exhibits a blue cone-free area about 100–150 μm in diameter in the central non-vascular region (Fig. 1A) (Wald, 1967). The rod-like blue cones in the fovea appear distributed in a rather cylindrical geometry. For a disc of 1 mm diameter, where the Haidinger's pattern is observed, only about 1000 blue cones are distributed among 200,000 clustered red and green cones (Bumsted & Hendrickson, 1999; Cornish et al., 2004; Curcio et al., 1991; Marcos & Burns, 1999). Then the blue cones appear isolated in the center of the retina with a very low density compared to the green and red ones, and isolated among clustered green and red cones. The maximum blue-cone density reaches about 1800 cones/mm^2 for eccentricities between 100 and 300 μm (Fig. 1B). The quasi regular arrangement of the red, green and blue cones in the center of the mosaic constitutes extra tangential sheaths, schematized by the pink lines in Fig. 1A and can act as pile-of-plate polarizers for oblique light travelling through the different interfaces (Hecht, 2002). So the difference between the transmitted intensities of orthogonally polarized beams reaching the chromophores can be increased. Moreover, to improve the acuity in the foveal area, the different rod-like cones in this region are narrower than those in the rest of the retina (Polyak, 1941) and quasi-parallel to each other (Heath & Walraven, 1970; Laties, Liebman, & Campbell, 1968), well suited to apply the Fresnel's laws The geometrical dimensions of the rod-like foveal cones are shown in Table 1.

Note that the disc with the 1 mm diameter where the brushes are observed is centered on a pit as shown in Fig. 2 with a radius of curvature of about 450 μm (Polyak, 1941). The pit induces a divergent lens effect introduced by Enoch and Hope. A mean ray schematized as in Fig. 1C falling on the cylindrical sheath of a cone at an incidence angle of 88° for instance, undergoes an extra deviation of about 2°. Moreover in this region of the retina the blue cones in the fovea are directly accessible to light without being obscured by inner retinal layers (Polyak, 1941).

2.3. Mechanism

To introduce the mechanism which removes the degeneracy of the symmetry in the blue sensitivity of the eye to polarized light, let us first consider an oblique blue ray passing through the center of the pupil (Fig. 1C). According to Fresnel's laws (see Appendix 1), the outer segments containing the chromophores of the blue cones in A or A′ can receive more oblique light than those in B or B′ for a polarized input along the *x*-axis. The corresponding extrinsic spatially distributed dichroism can be evaluated with indices of refraction of the cone membranes and of the surrounding cytoplasm comparable to the ones measured in frog rods (Liebman, Jagger, Kaplan, & Bargoot, 1974), i.e., 1.47 and 1.36 respectively. For instance with a ray impinging on an outer segment with an angle of incidence of 84°, a transmission difference of about 6% can be reached for orthogonal polarizations. Different types of oblique rays have to be considered. As shown in Fig. 1D, a second source of oblique rays labelled 2 is provided by the blue guided rays which escape from the different guiding cones and are partially recaptured (Chen & Makous, 1989). A third type labelled 3 comes from the quasi totality of blue rays guided without absorption by the dense green and red cones then falling on the fundus layers and partially reflected and scattered with a good preservation of the polarization (Delori & Pflibsen, 1989; van Blockland & van Norren, 1986). As seen below the quite low density of the blue cones in the center of the fovea leads to an additional blue specificity for the detection of oblique blue rays.

2.4. Brushes simulations based on oblique blue rays

We first fit the blue-cone distribution $D(r)$ of Fig. 1B versus the distance r from the foveal center. The cone-free area corresponds to $D(r) = 0$ for r values lower than 50 μm. For eccentricities ranging from 50 μm to 750 μm, which corresponds to the foveal center where the polarization pattern is observed, we use a ninth degree polynomial function fit from Mathematica (Wolfram Research, Urbana, Illinois, USA) for the cones distribution shown in Fig. 1B. For a stimulus polarized along the *x*-axis (Fig. 1C) the excitation due to an oblique ray impinging on the cones localized at points A or A′ in the incidence plane is proportional to the parallel Fresnel coefficient $T_{//}(i)$, where i is the angle of incidence on the cones (see Appendix 1). The excitation of the cones at points B and B′ is proportional to $T_{\perp}(i)$, the corresponding perpendicular Fresnel coefficient. For a cone located at the angle θ from the *x*-axis, the intensity entering into the cone is proportional to $(T_{//}(i)\cos^2\theta + T_{\perp}(i)\sin^2\theta)$ giving transmission values varying from $T_{\perp}$ to $T_{//}$. The response of the retina to the different oblique ray contributions for the blue cones in the central region with their distribution $D(r)$ is represented by $R \propto D(r)(T_{//}(i)\cos^2\theta + T_{\perp}(i)\sin^2\theta)$. Introducing both the polarized independent guided blue light also proportional to $D(r)$ and the oblique part subject to Fresnel's laws, lead to the typical blue-dark patterns of Fig. 3 for three axis orientations of the incident blue light polarization. These patterns are similar to the blue-dark patterns that can be readily observed

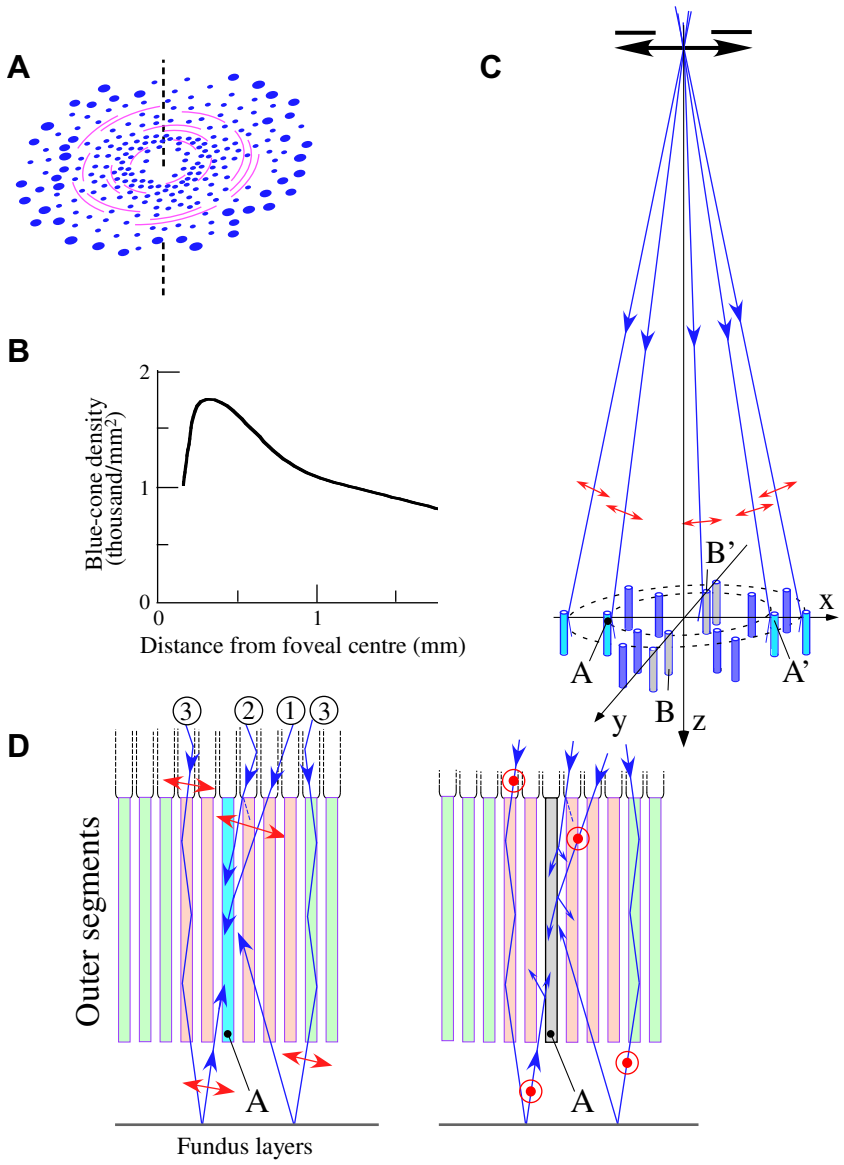

Fig. 1. (A) Schematic representation of the blue-cone distribution on the fovea. Note the blue cone-free area at the center of the fovea. The partial regular arrangement of the red, green and blue cones in the center of the mosaic can constitute extra tangential sheaths, schematized by the pink lines, which act as pile-of-plate polarizers for oblique light. (B) Blue-cone density versus the distance from the foveal center (Bumsted & Hendrickson, 1999; Cornish et al., 2004; Curcio et al., 1991). (C) Oblique mean polarized blue rays passing through the center of the pupil impinging on the outer blue segments which contain the chromophores. The polarization along the x axis is more efficiently transmitted for the A and A′ cones than for the B and B' cones according to Fresnel's laws. (D) The three main contributions of blue oblique rays reaching the blue cone A in the fovea transmitted according to Fresnel's laws with the polarization in the plane of incidence (left: higher efficiency) and perpendicular to the plane of incidence (right: lower efficiency). A blue ray guided by a blue cone is progressively absorbed along its outer segment independently of its polarization. However, most of the blue rays guided by the dense green and red cones are not absorbed and are partially reflected by the fundus layers with high preservation of their polarization, reinforcing the total blue oblique rays. (For interpretation of the references to colour in this figure legend, the reader is referred to the web version of this article.)

Table 1
Foveal cone dimensions (Polyak, 1941). The space between the cone axes is 2.3 μm, and the cone sheaths are of 0.5 μm thickness. Outside the central fovea the inner segment diameter is larger by a factor of 2–3 and the outer segments become conical.

Part of the cones	Diameter (μm)	Length (μm)
Inner segment	1.8	25
Outer segment	1.3	40

in vivo by gazing at a liquid crystal screen of a desktop computer. These screens provide linearly polarized light often at 45° from the vertical. Using a blue filter and a simple rotating 25 μm thick cellophane sheet which acts as a half-wave plate, one can observe patterns in a visual angle of about 3°, evolving around the dark Maxwell fixation point (Maxwell, 1856) which is linked to the absence of blue cones at the center of the fovea (Magnussen, Spillmann, Stürzel, & Werner, 2001).

2.5. Contrast estimation of the patterns

To qualify the polarization brushes observed through a dark blue filter, let us consider the Michelson contrast commonly used for patterns with bright and dark features. Here for an incident light polarized along the *x*-axis of Fig. 1C, let us introduce I_x and I_y, the intensities of the light detected by the outer blue segments along the *x* and *y* axes respectively. The Michelson contrast of Haidinger's patterns can be defined as $C = (I_x - I_y)/(I_x + I_y)$. The difference $(I_x - I_y)$ comes only from the oblique blue rays transmitted

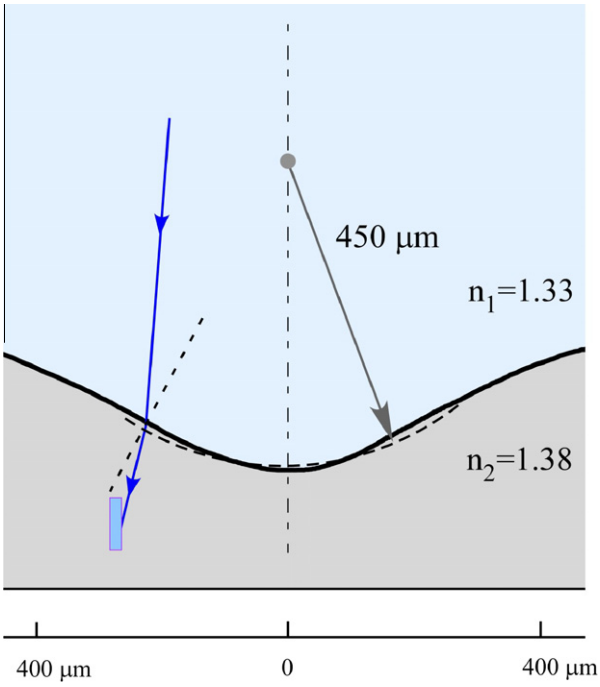

Fig. 2. Scheme of the central foveal pit showing the divergent lens effect (Enoch & Hope, 1973) for light impinging on the sheath of an outer segment.

according to Fresnel's laws and the sum $I_x + I_y$ represents the total blue intensity including the guided part which is independent of the polarization, and the unguided oblique part which is polarization dependent. To estimate the Michelson contrast we have to evaluate both parts.

First let us recall that taking account of the cone diameters given in Table 1 and of their densities, for any light impinging on the inner segments of the fovea leads to a 70% guided part and to a 30% unguided oblique part falling on the inner segments sheets. The absorption of the guided photons propagating in their own cones may reach 75% along the 40 μm length of the outer segments, the typical absorption coefficient being equal to 0.035 μm^{-1}. For the blue cones with their low density, the detected guided polarization independent contribution for a central 1 mm diameter disc reaches only 0.18% of the total blue input.

For the oblique blue rays which have to obey to Fresnel's laws, the low density of the blue cones implies a blue specificity as these cones are isolated among clustered red and green cones. Indeed the mean-free path of the oblique blue rays is longer by about a factor two compared to the red or green rays. Moreover as a blue cone is isolated in the mosaic its individual cylindrical cross section is estimated to be twice that of a red or green cone embedded in a cluster. Note that in addition the absorption curve of the blue retinal chromophore is well separated from that of the red and green chromophore curves which largely overlap. So the guided transmitted part reaching the fundus is about four times larger for the blue light than for the green and red lights, with a higher preservation of the polarization as observed by van Blockland and van Norren (1986).

For the different blue oblique rays, the mean cross section of the cones is estimated to be 0.7 and the light detection yield of a cone to be 0.4, if we take into account the reflection on the sheaths and the shorter oblique absorption length. For the 30% oblique rays falling on the inner sheaths, 0.04% is then detected. From the 30% escaped oblique rays originating from the 70% initially guided light, 0.03% is also detected. Considering a reflectance of 0.2, the detected blue oblique rays from the fundus layers give a contribution of 0.03%. The total blue oblique light detected intensity amounts to 0.1%. For a mean Fresnel's transmission difference of about 0.07, the expected contrast in Haidinger's pattern is then found to be 2.5%. This contrast in the blue part of the spectrum is reduced on the margin of the pit where the cone geometries are changed reducing the efficiency of Fresnel' laws discrimination, their outer segments becoming conical while the rod density increases. Furthermore in this region, the cones become obscured by the thicker inner retinal layers (Polyak, 1941). In the green and red parts of the spectrum, for the green and red photons falling on the center of the fovea, the relative contributions of the corresponding different oblique rays impinging on the clustered green and red outer cones are reduced by a factor from 3 to 4 as discussed above. The resulting contrast is then reduced to less than 1%, i.e., below the eye threshold detection (Hubel, 1988). Hence the mechanism at the origin of Haidinger's patterns appears restricted to the blue–violet part of the spectrum as observed.

3. Experiment 1: the artificial eye model system

3.1. Apparatus

Our proposed mechanism can be confirmed by the construction of an artificial eye which includes the three basic functions as shown in Fig. 4A. A lens bends the incoming polarized light in place of the cornea and the lens. A glass cylinder representing the cone membranes differentially transmits the oblique light according to Fresnel's laws along the x and y axes. A blue mosaic on a screen, representing the chromophores of the real cone distribution, collects the transmitted blue light beyond the interface, which is recorded by a camera. The photograph of a part of the artificial eye is shown in Fig. 5. The auxiliary laser spot shows the mimicking eye movements (Hafed, Goffard, & Krauzlis, 2009; Martinez-Conde, Maknik, & Hubel, 2002), activated by two motors. An extra birefringent plate can be added in front of the lens to simulate the ef-

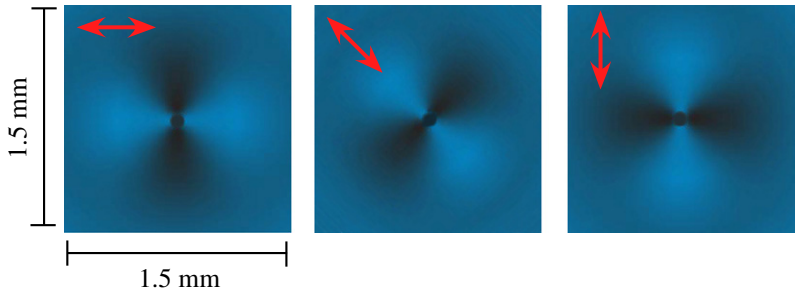

Fig. 3. Typical simulations of the blue-dark Haidinger's brushes using the blue cone description of Fig. 1B. Three polarization orientations of the incoming light are selected: 0°, 45° and 90°. The whole human fovea is about 1.5 mm in diameter, corresponding to a visual angle of 5°. (For interpretation of the references to colour in this figure legend, the reader is referred to the web version of this article.)

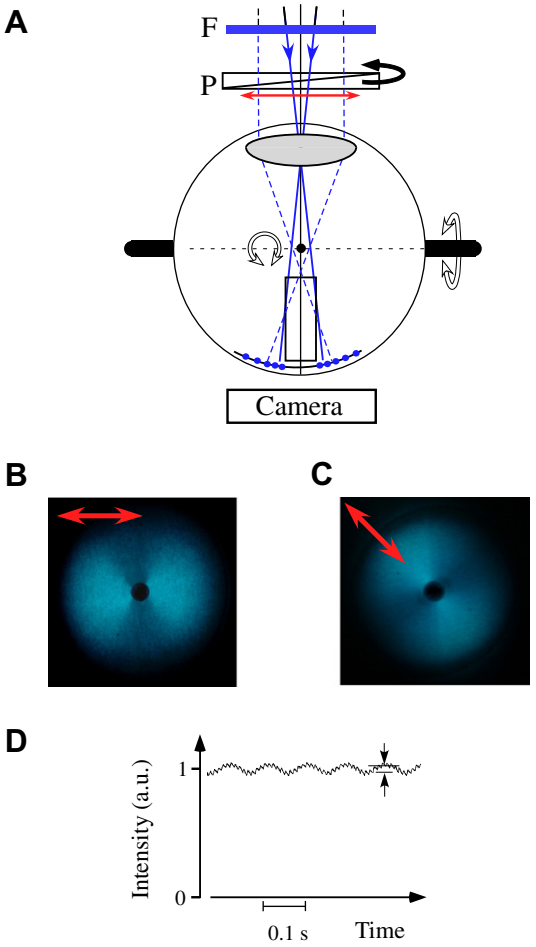

Fig. 4. An artificial eye to observe Haidinger-like patterns. (A) Schematic of the experimental system. The polarization of the input light can be adjusted and rotated thanks to a polarizer P. The focal length of the lens is 20 mm. A glass cylinder with a 4 mm diameter mimics a cylindrical distribution of rod-like cones around the center of the fovea for the oblique rays. The oblique transmitted blue light selected by a blue filter F, obeying Fresnel's laws is collected through a blue mosaic representing the real blue-cone distribution. Extra birefringence plates representing the corneal retardances and cylindrical lenses introducing possible astigmatisms are not represented here. The whole system can be moved with motors around two orthogonal rotation axes to mimic small eye movements (see also Fig. 5). (B and C) experimental patterns photographed by the camera for 0° and 45° orientations of the polarization respectively. (D) Experimental measurement of the pattern contrast. The rotation frequency of the incident polarization is 5 Hz. (For interpretation of the references to colour in this figure legend, the reader is referred to the web version of this article.)

fect of a possible corneal retardance (Greenfield, Knighton, & Huang, 2000). Moreover a possible astigmatism can also be introduced by interposing an extra cylindrical lens in front of the eye lens.

3.2. Results

The experimental patterns can then be photographed, as shown in Fig. 4B and C for the corresponding 0° and 45° angles of the polarization orientations taken in the simulations. The contrast of the pattern when the light polarization is rotated can be recorded using a small detector in place of the camera. Fig. 4D shows a typical experimental contrast of about 3%, in qualitative agreement with the simulations and the *in vivo* observations. Adding some extra green and red light on the screen, the blue part of the spectrum remains enhanced along the polarization axis of the light, while on the perpendicular direction the yellow color appears, exhibiting

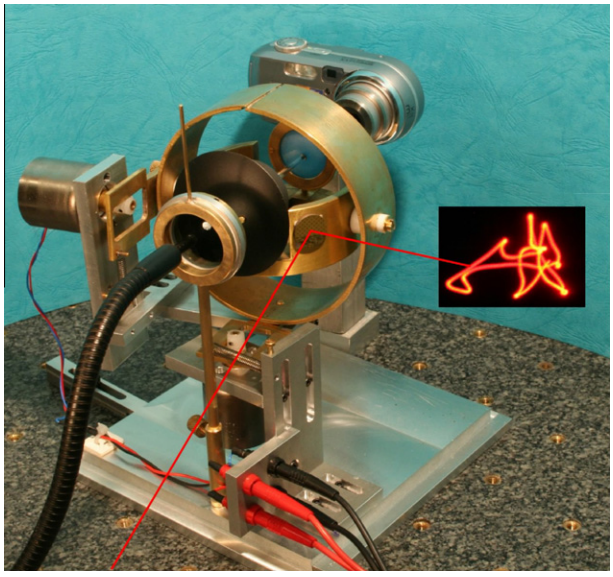

Fig. 5. Photograph of a part of the artificial eye corresponding to the scheme of Fig. 4A.

then the usual blue–yellow brushes observed with white light. Note that the observed patterns remain stable in presence of the artificial eye movements just as for the real eye where the brushes are highly stable on the fovea. Adding an extra birefringent plate in front of the lens only reduces the pattern contrast. No noticeable modification is introduced by interposing a cylindrical lens, i.e. astigmatism, as confirmed by the direct *in vivo* observations of the Haidinger's patterns.

4. Experiment 2: measurement of the creating and erasing time

4.1. Introduction

The randomly-aligned anisotropic cone chromophores play no role in the production of the polarized patterns in human vision. However a built-in paradox remains: if the polarized stimulus rotation is stopped, so as to better examine the pattern, the image fades and disappears slowly in about 3 s due to neural adaptation (Martinez-Conde et al., 2002), but if the polarization direction is changed abruptly, the image reappears quasi-instantaneously. A direct *in vivo* test by observing Haidinger's brushes with a computer screen allows us to measure the extra fast creating and erasing time characterizing the entoptic pattern dynamics, either by rotation or by flip–flop polarization changes. By moving electromechanically back and forth in a horizontal direction a half-wave plate oriented such as to switch the light polarization of the computer screen by 90°, a human is able to observe the 90° flip–flop polarization pattern changes for frequencies reaching 8–10 Hz. This 0.1 s fast pattern creating and erasing time could correspond to opsin activation (Martinez-Conde et al., 2002) and can be tested in an *in vitro* experiment on the same retinal chromophore with a bacteriorhodopsin film.

4.2. Apparatus

The bacteriorhodopsin protein contains the same retinal which activates an opsin of the same family with different functions and phototransductions, with a similar seven α-helical transmembrane architecture (Oesterhelt et al., 2000; Palczewski, 2006). The sample of bacteriorhodopsin was purchased from Munich Innovative Biomaterials (Munich, Germany). Its thickness is 80 μm and its optical

density is about 3 at 570 nm. The sample is irradiated with a 150 μW polarized stimulus (S) provided by a double frequency Nd:YAG laser at 532 nm beam. A weak beam (*p*) at the same wavelength, with a rotating polarization, probes the interaction zone (see insert in Fig. 6).

4.3. Results

Firstly in the absence of the stimulus, the probe (*p*) with a rotating linear polarization is transmitted with a constant intensity noted 1 in arbitrary units (lower trace in Fig. 6A). Secondly in the presence of the stimulus polarized along one axis, a small intrinsic molecular dichroism is induced in the film according to Malus' law and is detected by the rotating probe (upper trace in Fig. 6A). The bleaching of the retinal chromophore along the polarization axis of the stimulus leads to a higher transmission of the probe. The maxima of the oscillations correspond to probe and stimulus with parallel polarizations. An exponential decrease is observed when the stimulus is suppressed. Note that this experimental response is independent of the polarization orientation of the stimulus, the retinal molecules being randomly distributed as in the human retina. This intrinsic molecular dichroism cannot be at the origin of the Haidinger's patterns but governs their creating and erasing time.

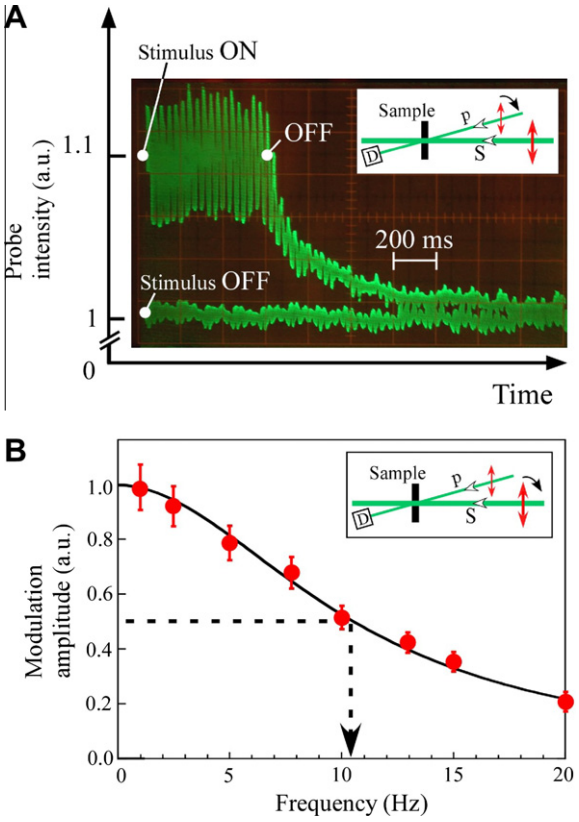

Fig. 6. *In vitro* experimental measurement of the fast erasing time of photopigments. (A) Firstly a probe (p) with a rotating linear polarization is transmitted with a constant intensity noted 1 in arbitrary units (lower trace). Secondly in the presence of a stimulus (S) polarized along one axis, a small intrinsic molecular dichroism is induced (upper trace). The maxima of the oscillations correspond to probe and stimulus with parallel polarizations. An exponential decrease is observed when the stimulus is stopped. (B) Measurement of the lifetime of the angular bleaching using rotation polarization spectroscopy. The polarization of the probe is now fixed, while the rotation frequency of the stimulus polarization is increased. For too-high frequencies the probe signal vanishes, the bleaching being the same in all directions. The full line represents a lorentzian fit corresponding here to a lifetime value of 95 ms.

This angular bleaching offers a powerful tool for measuring the associated lifetime using rotating polarization spectroscopy (Emile, Bretenaker, & Le Floch, 1995), which is well adapted to detect a dichroism induced by a linearly polarized light beam in molecules. Here, the sample of bacteriorhodopsin is submitted to a rotating polarization stimulus, the dichroism being detected by a fixed polarization probe. Among the randomly dichroic distributed molecules, those whose axes are parallel to the electric field stimulus are more bleached than those orthogonal to it, in agreement with Malus' law. When the frequency of the polarization rotation is increased up to 20 Hz, the modulation of the probe signal is reduced by a factor of 5. The experimental results shown in Fig. 6B were fitted with the expected Lorentzian function leading to a lifetime value of 95 ms, in the same range as the value observed for rhodopsin in our *in vivo* eye pattern rotation measurements.

This rapid response of the patterns could allow a human, with the naked eye, to compare two successive orientations of the polarization with a precision of about $\pm 5^{\circ}$, to read hidden information coded via different axes of polarization or even to detect directly quantum entanglement as recently discussed (Sekatski, Brunner, Branciard, Gisin, & Simon, 2009).

5. General discussion and conclusion

One may wonder if the Haidinger's patterns are the same for the right and for the left eye. For one eye, the propeller-like image rotates more regularly around its more circular fixation spot. For the other eye, the dark axis appears more diffuse in one direction, generally the vertical one. Direct post-mortem observations of blue cones of the retina using labelling methods (Bumsted & Hendrickson, 1999) have indeed shown that although the blue cone-free area is clearly defined, in some foveas, the shape of the cone-free area tends to be more oval than round, with the oval aligned along the horizontal meridian. These symmetry differences between the blue-cone distributions in the two eyes could affect the quality of the two patterns. *In vivo* rotating pattern differences can be detected in white and blue light observations for the two eyes. Such asymmetry of the eyes has earlier been evoked by Helmholtz himself noting that the center of the dark brush is much darker in his left eye than in his other eye (von Helmholtz, 1962). Moreover, as suggested earlier by Newton (Newton, 1979) surprisingly enough, the *corpus callosum* in the brain has to cement together the right and left halves of the visual field of each eye (Hubel, 1988; Perenin & Vadot, 1981), along a line passing vertically, exactly through each foveal center. Intuitively the necessary connectivity in the nervous system could be easier to realize for the eye with the more circular blue-cone distribution in its fovea and could establish the eye dominancy. We have tested this hypothesis on 20 observers (12 right-eye dominant and 8 left-eye dominant, see Appendix 2) looking at a polarized screen through a blue filter and a rotating half-wave plate and found in all cases, that the eye with the more regular and less diffused rotating Haidinger's pattern around a more circular darker center seems to be the dominant eye. Although the test has been performed on only 20 observers, the polarization pattern appears to be a sensitive probe for the poorly understood phenomenon of eye dominancy (Coren & Porac, 1976; Crovitz, 1961; Roth, Lora, & Heilman, 2002) which could to be linked to the cone distribution with a more circular blue cone-free area in one fovea.

The possibility of direct perception by the brain of the polarization sense in human eyes and the understanding of the fundamental mechanisms involved, with their temporal and asymmetrical properties, may suggest new tests for some retinal diseases (Cepko, 2000; Lewis & et al., 1977; Perenin & Vadot, 1981) and naked eye

applications such as ocular imaging, detecting quantum phenomena (Sekatski et al., 2009) and coding information.

Acknowledgments

We like to thank W. Makous and R.W. Boyd (Rochester University) for their helpful suggestions; D.E. Nilsson (Lund University) and D. van Norren (Utrecht University) for their fruitful discussions concerning the guided and oblique rays; I. McAllister (LEI Perth) for comments on foveal retinoschisis disease, A. Carré, C. Hamel and L. Frein for their technical assistance. This work was supported by the Contrat Plan Etat-Région PONANT.

Appendix 1. Fresnel's coefficients

When light moves from a medium of a given refractive index n_1 into a second medium with a refractive index n_2, both reflection and refraction may occur. The transmittance at the interface defined as the ratio of the transmitted to the incident flux is defined as, for the electric field parallel to the plane of incidence:

$$T_{\parallel} = \frac{\sin 2i \sin 2r}{\sin^2(i+r)\cos^2(i-r)},$$

where i and r are the angles of incidence and of refraction respectively, governed by the Snell's law ($n_1 \sin i = n_2 \sin r$).

For the electric field perpendicular to the plane of incidence, the transmittance is:

$$T_{\perp} = \frac{\sin 2i \sin 2r}{\sin^2(i+r)}$$

Appendix 2. Eye dominant determination

The tendency to prefer visual input from one eye rather than the other is determined by means of different methods. In standard sighting tests, the observer can extend one arm, form a small circular opening with the thumb and index finger and then with both eyes opened view a distant object through the opening. The observer then alternates closing one eye then the other to determine which eye is viewing the object. Approximately two-thirds of the population are right-eye dominant.

References

Born, M., & Wolf, E. (1999). *Principles of optics*. Cambridge: Cambridge University Press.

Brewster, D. (1859). Sur les houppes colorées ou secteurs de Haidinger. *Comptes rendus de l'Académie des Sciences, 48*, 614–618. (Brewster reported that four patients whose lenses have been removed were still able to see the Haidinger's brushes).

Bumsted, K., & Hendrickson, A. (1999). Distribution and development of short-wavelength cones differ between macaca monkey and human fovea. *Journal of Comparative Neurology, 403*, 502–516.

Cepko, C. (2000). Giving in to the blues. *Nature Genetics, 24*, 99–100.

Chen, B., & Makous, W. (1989). Light capture by human cones. *Journal of Physiology, 414*, 89–109.

Coren, S., & Porac, C. (1976). Size accentuation in the dominant eye. *Nature, 260*, 527–528.

Cornish, E. E., Hendrickson, A. E., & Provis, J. M. (2004). Distribution of short-wavelength-sensitive cones in human fetal and postnatal retina: Early development of spatial order and density profile. *Vision Research, 44*, 2019–2026.

Crovitz, H. F. (1961). Differential acuity of the two eyes and the problem of ocular dominances. *Science, 134*, 614.

Curcio, C. A., Allen, K. A., Sloan, K. R., Lerea, C. L., Hurley, J. B., Klock, I. B., et al. (1991). Distribution and morphology of human cone photoreceptors stained with anti-blue opsin. *Journal of Comparative Neurology, 312*, 610–624.

Dacke, M., Nilsson, D. E., Scholtz, C. H., Byrne, M., & Warrant, E. J. (2003). Insect orientation to polarized moonlight. *Nature, 424*, 33.

Delori, F. C., & Pflibsen, K. P. (1989). Spectral reflectance of the human ocular fundus. *Applied Optics, 28*, 1061–1077.

Emile, O., Bretenaker, F., & Le Floch, A. (1995). Rotating polarization-induced resonance in atoms and molecules. *Physical Review Letters, 75*, 1907–1910.

Enoch, J. M., & Hope, G. M. (1973). Directional sensitivity of the foveal and parafoveal retina. *Investigative Ophthalmology, 12*, 497–503.

Greenfield, D. S., Knighton, R. W., & Huang, X. R. (2000). Effect of corneal polarization axis on assessment of retinal nerve fiber layer thickness by scanning laser polarimetry. *American Journal of Ophthalmology, 129*, 715–722.

Hafed, Z. M., Goffard, L., & Krauzlis, R. J. (2009). A neural mechanism for microsaccade generation in the primate superior colliculus. *Science, 323*, 940–943.

Haidinger, H. (1844). In J. C. Poggendorf (Ed.), *Annalen der Physik und Chemie* (Vol. 63, p. 29).

Heath, G., & Walraven, P. (1970). Receptor orientations in the central region. *Journal of the Optical Society of America, 60*, 733.

Hecht, E. (2002). *Optics* (4th ed.). Addison Wesley. p. 349.

Heinze, S., & Homberg, U. (2007). Maplike representation of celestial *E*-vector orientations in the brain of an insect. *Science, 315*, 995–997.

Horwáth, G., & Varjú, D. (2004). *Polarized light in animal vision: Polarization patterns in nature* (pp. 355–361). Berlin: Springer-Verlag.

Hubel, D. H. (1988). *Eye, brain, and vision*. New York: W.H. Freeman.

Laties, A. M., Liebman, P. A., & Campbell, C. E. M. (1968). Photoreceptor orientation in the primate eye. *Nature, 218*, 172–173.

Lewis, R. A. et al. (1977). Familial foveal retinoschisis. *Archives of Ophthalmology, 95*, 1190–1196.

Liebman, P. A., Jagger, W. S., Kaplan, M. W., & Bargoot, F. G. (1974). Membrane structure changes in rod outer segments associated with rhodopsin bleaching. *Nature, 251*, 31–36.

Magnussen, S., Spillmann, L., Stürzel, F., & Werner, J. S. (2001). Filling-in of the foveal blue scotoma. *Vision Research, 41*, 2961–2967.

Marcos, S., & Burns, S. A. (1999). Cone spacing and waveguide properties from cone directionality measurements. *Journal of the Optical Society of America A, 16*, 995–1004.

Martinez-Conde, S., Maknik, S. L., & Hubel, D. H. (2002). The function of bursts of spikes during visual fixation in the awake primate lateral geniculate nucleus and primary visual cortex. *Proceedings of the National Academy of Sciences (USA), 99*, 13920–13925.

Maxwell, J. C. (1856). On the unequal sensibility of the foramen centrale to light of different colours. *Athenaeum, 1505*, 1093.

Newton, I. (1979). *Optics* (Query 15). New York: Dover Publications.

Oesterhelt, F., Oesterhelt, D., Pfeiffer, M., Engel, A., Gaub, H. E., & Müller, D. J. (2000). Unfolding pathways of individual bacteriorhodopsins. *Science, 288*, 143–146.

Osterberg, G. (1935). Topography of the layer of rods and cones in the human retina. *Acta Ophthalmologica, 6*(Suppl), 1–102.

Oyster, C. W. (1999). *The human eye, structure and function*. Sunderland: Sinauer.

Palczewski, K. G. (2006). G protein–coupled receptor rhodopsin. *Annual Review of Biochemistry, 75*, 743–767.

Perenin, M. T., & Vadot, E. (1981). Macular sparing investigated by means of Haidinger brushes. *British Journal of Ophthalmology, 65*, 429–435.

Polyak, S. L. (1941). *The retina*. Chicago: University of Chicago Press.

Raman, C. V. (1965). The new physiology of vision – Chapter IX. The structure of the fovea. *Proceedings of the Indian Academy of Science, A61*, 258–261.

Rodieck, R. W. (1998). *The first steps in seeing*. Sunderland: Sinauer.

Roth, H. L., Lora, A. N., & Heilman, K. M. (2002). Effects of monocular viewing and eye dominance on spatial attention. *Brain, 125*, 2023–2035.

Sekatski, P., Brunner, N., Branciard, C., Gisin, N., & Simon, C. (2009). Towards quantum experiments with human eyes as detectors based on cloning via stimulated emission. *Physical Review Letters, 103*, 113601.

Stokes, G. G. (1883). On Haidinger's brushes. *Mathematical and Physical papers* 2. Cambridge University Press (pp. 362–364).

van Blockland, G. J., & van Norren, D. (1986). Intensity and polarization of light scattered at small angles from the human fovea. *Vision Research, 26*, 485–494.

von Frisch, K. (1967). *The dance language and orientation of bees*. Cambridge: Harvard University Press.

von Helmholtz, H. (1962). In J. P. C. Southall (Ed.), *Treatise on physiological optics* (Vol. II, p. 301). New York: Dover.

Wald, G. (1967). The molecular basis of visual excitation. *Nobel lecture*.

Wehner, R., & Müller, M. (2006). The significance of direct sunlight and polarized skylight in the ant's celestial system of navigation. *Proceedings of the National Academy of Science, 103*, 12575–12579.